that in the case of **1** and **2** the absence of electrolyte in the $[Me_3N(CH_2)_4NMe_3][Ni(dmit)_2]_2$ solution results in a higher resistivity and thus increases the electric potential of the anode. This yields a higher oxidizing ability of the anode.

The latter theory is supported by the existence of the salts $[HNMe_3]_2[Ni(dmit)_2]_5 \cdot 2CH_3CN$ and $[H_3NMe]_2[Ni(dmit)_2]_5 \cdot 2CH_3CN$, which have recently been reported.[26,27] These two *semi*conductors were obtained *together* with the conducting 1:2 salts $[HNMe_3][Ni(dmit)_2]_2$[5] and $[H_3NMe][Ni(dmit)_2]_2$[27], which advocates the idea that it is the electrochemical oxidation conditions that determine the degree of oxidation, rather than the nature of the closed-shell cation. An important conclusion resulting from this analysis is that changing the electrooxidation conditions, e.g. by choosing a better a solvent for $[Me_3N(CH_2)_4NMe_3][Ni(dmit)_2]_2$, might indeed yield the desired oxidation state of $Ni^{3.5+}$. This means that although the goal of mimicking the crystal structure of $[Me_4N][Ni(dmit)_2]_2$ is not yet reached, a correct modification in the electrocrystallization process could result in a compound with the stoichiometry $[Me_3N(CH_2)_4NMe_3][Ni(dmit)_2]_4$. A salt with this formula would obviously have a greater possibility of having a packing mode similar to that of the superconducting $[Me_4N][Ni(dmit)_2]_2$.

Acknowledgment. We thank Ms. B. Pomarède and Ms. Dr. L. Valade for performing the conductivity measurements. We are indebted to Dr. J.-P. Legros for automatic X-ray diffractometer use, for providing information on and the coordinates of $[H_3NMe]_2[Ni(dmit)_2]_5 \cdot 2CH_3CN$ and $[HNMe_3]_2[Ni(dmit)_2]_5 \cdot 2CH_3CN$, and for his stimulating interest. Mr. S. Gorter collected the X-ray diffraction data for **1**. We are grateful to NWO (Nederlandse stichting voor Wetenschappelijk Onderzoek) and to the CNRS (Centre National de la Recherche Scientifique) in Paris for financial support. This research was in part sponsored by the Werkgroep Fundamenteel Materialen Onderzoek (WFMO).

Supplementary Material Available: Tables of crystal data and details of the structure determinations, atomic coordinates for the hydrogen atoms, thermal parameters of all non-hydrogen atoms, and all bond distances and angles for **1** and **2** (39 pages); listings of calculated and observed structure factors (78 pages). Ordering information is given on any current masthead page.

Contribution from the Department of Chemistry, University of California, Davis, California 95616, and Institute of Chemistry, University of Wrocław, Wrocław, Poland

Chemistry of Iron Oxophlorins. 1. ^{1}H NMR and Structural Studies of Five-Coordinate Iron(III) Complexes

Alan L. Balch,*,† Lechosław Latos-Grażyński,‡ Bruce C. Noll,† Marilyn M. Olmstead,† and Edward P. Zovinka†

Received February 5, 1992

As part of a series of studies to understand the role of iron oxophlorin complexes in oxidative heme destruction, the spectroscopic, chemical, and structural features of a group of dioxygen-stable iron(III) complexes of octaethyloxophlorin are reported. Protonation or coordination of the meso oxygen of the oxophlorin ligand appears to stabilize these iron complexes and prevents their conversion to verdoheme through oxidation by molecular oxygen. The ^{1}H NMR spectrum of dimeric $[Fe^{III}(OEPO)]_2$ (where OEPO is the trianion of octaethyloxophlorin, **1**), is presented and analyzed. The presence of two paramagnetic centers produce marked variation in line widths and T_1's for the methylene protons. $[Fe^{III}(OEPO)]_2$ is cleaved by protic acids (HX) to form high-spin, five-coordinate $[XFe^{III}(OEPOH)]$, whose ^{1}H NMR and electron paramagnetic resonance spectra are analyzed. As a model for $[XFe^{III}(OEPOH)]$, the complex $[ClFe^{II}(OEPOAc)]$ (where the meso hydroxyl group has been acetylated) has been prepared and characterized by its ^{1}H NMR spectrum. The X-ray crystal structure of $[ClFe^{III}(OEPOAc)\cdot CH_2Cl_2$ shows that the iron is five-coordinate with structural parameters consistent with high-spin ($S = {}^5/_2$) electronic structure. Crystals of $C_{39}H_{48}Cl_3FeN_4O_2$ form in the triclinic space group $P\bar{1}$ with $a = 10.238$ (2) Å, $b = 13.301$ (2) Å, $c = 15.088$ (3) Å, $\alpha = 77.610$ (2)°, $\beta = 71.820$ (2)°, and $\gamma = 75.430$ (2)°, at 130 K with $Z = 2$. Refinement of 4577 reflections with 456 parameters yielded $R = 0.051$ and $R_w = 0.053$. The environment about the acetoxy substituent is crowded, and restricted rotation at that site produces two isomers that are observed in solution.

Introduction

Oxophlorins (or oxyporphyrins), **1**, are porphyrin derivatives that have been oxygenated at one meso position.[1,2] Two tautomeric forms are possible: one, **1a**, with a hydroxyl group at the meso position, the other, **1b**, with a carbonyl group at that site. An iron oxophlorin complex is an intermediate in the conversion of heme to biliverdin in both the in vivo process that is catalyzed by heme oxygenase and the in vitro model system known as coupled oxidation (Scheme I; iron ligation and oxidation states unspecified, other structures have been proposed for verdoheme).[3,4] Coordinated iron is critically important in both processes. Por-

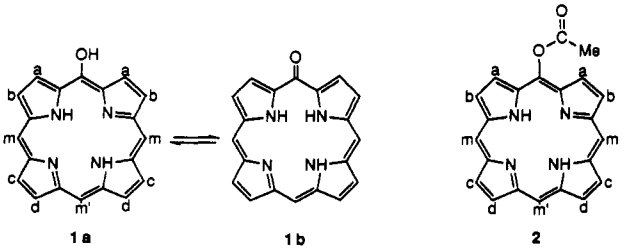

1a **1b** **2**

Scheme I

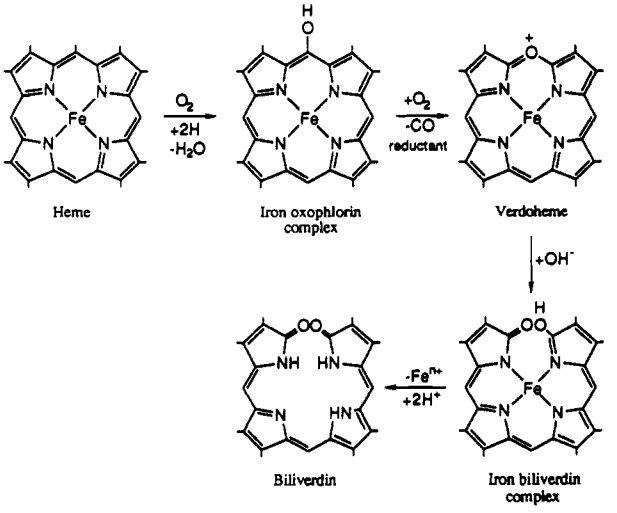

† University of California, Davis.
‡ University of Wrocław, Poland.

Table I. ^{1}H NMR Parameters for Iron Octaethylporphyrin Complexes

compound	spin state	coordination no.	meso	methylene	methyl	solvent	T, C°	ref
$ClFe^{III}(OEP)$	$^5/_2$	5	−56.1	44.5, 40.9	6.7	CD_2Cl_2	25	*a*
$O\{Fe^{III}(OEP)\}_2$	$^5/_2$[e]	5	5.5	6.06, 5.10	1.75	$CDCl_3$	29	*b*
$\{OFe^{III}(OEP)\}_2$	$^5/_2$[e]	5	−2.3	8.85, 6.26	1.74	toluene-d_8	−75	*c*
(*N*-MeIm)Fe^{IV}=O(OEP)	1	6	15	0	3.2	toluene-d_8	−33	*c*
$Fe^{II}(OEP)$	1	4	76.3	33.8	12.9	benzene-d_6	25	*d*

[a] Morishima, I.; Kitagawa, S.; Matsuki, E.; Inubushi, T. *J. Am. Chem. Soc.* **1980**, *102*, 2429. [b] La Mar, G. N.; Eaton, G. R.; Holm, R. H.; Walker, F. A. *J. Am. Chem. Soc.* **1973**, *95*, 63. [c] Chin, D. H.; La Mar, G. N.; Balch, A. L. *J. Am. Chem. Soc.* **1980**, *102*, 4344. [d] Strauss, S. H.; Silver, M. E.; Long, K. M.; Thompson, R. G.; Hudgens, R. A.; Spartalian, K.; Ibers, J. A. *J. Am. Chem. Soc.* **1985**, *107*, 4207. [e] Antiferromagnetically coupled.

Table II. ^{1}H NMR Parameters for Iron Complexes

compound	solvent	temp, °C	m	m′	methylenes	methyls	HO–
$ClFe^{III}(OEP)$	CD_2Cl_2	25	−56.0		44.0, 40.5	6.7	
$[Fe^{III}(OEPO)]_2$, **3**	CD_2Cl_2	28	−98.4	−28.0	18.0, 23.2, 28.8, 30.0, 31.8, 33.6, 37.1, 39.1	−1.4, 4.1, 4.4, 5.2	
$[Fe^{III}$(Etio I O)$]_2$	$CDCl_3$	25	−97.4	28.0	14.7, 18.4, 18.7, 23.2, 29.2, 30.1, 31.9, 33.0, 34.3, 40.5, 44.7	54.5, 53.9, 42.3, 40.9, 40.0, 21.1	
[$BrFe^{III}$(Etio I OH)]	$CDCl_3$	25	−91.5	−78.1	28.8, 34.3, 37.8, 39.0, 41.3, 42.2, 43.3, 45.3	46.4, 48.0, 53.5, 58.5	20.1[a]
$ClFe^{III}$(OEPOH)	$CDCl_3$	25	−91.9	−78.3	34.0, 37.2, 40.3, 41.5, 43.1, 46.1		26.5
$BrFe^{III}$(OEPOH)	$CDCl_3$	25	−93.2	−78.8	35.7, 39.1, 42.2, 43.4, 42.2, 48.6	1.5, 7.1, 7.4, 8.7	28.2
$(CF_3CO_2)Fe^{III}$(OEPOH)	CD_2Cl_2	23	−71.7	−66.3	36.2, 39.0, 42.7, 43.6, 44.3, 46.2, 49.6, 53.4		28.2
$ClFe^{III}$(OEPOAc)	$CDCl_3$	23	−71.7	−66.3	36.2, 39.2, 39.7, 40.8, 41.4, 42.5, 44.0, 45.9		
			−60.9	−55.5			
$BrFe^{III}$(OEPOAc)	CD_2Cl_2	23	−70.2, −65.5	−61.8, −55.7	38.2, 39.0, 40.6, 41.7, 42.8, 43.5, 45.5, 46.9, 47.8, 48.4	7.1, 7.7	

[a] At −20 °C.

phyrins themselves are not nearly as susceptible to the initial meso oxygenation as are the iron complexes. While heme (iron protoporphyrin) is readily degraded by heme oxygenase, tin, manganese, and zinc hemes are competitive inhibitors of this enzyme,[5] and tin protoporphyrin IX has been used in the clinical treatment of hyperbilirubinemia.[6] However, much remains to be understood about the role of iron in the process of heme degradation. To this end we have begun to examine the coordination chemistry of one of the intermediates, the iron oxophlorins.

In examining the binding of metal ions to oxophlorins, one has all of the problems encountered in porphyrin chemistry. These include the need to identify the axial ligation and metal ion spin state and to establish the overall oxidation level (that is total electron count) and the oxidation states (that is the apportionment of electrons between metal and ligands). In the last issue, the fact that oxophlorins are readily oxidized[7,8] means that complexes involving the ligand in radical form are more easily obtained for oxophlorins that for porphyrins. As an additional complication, the protonation state of the meso oxygen needs to be identified. The oxophlorin ligand can coordinate as a dianion with a meso hydroxyl group or it may bond as a trianion. In order to distinguish between these, we have employed the acetoxy derivative **2** (a–d = ethyl, m and m′ = hydrogen) as a model for coordination as a porphyrinic dianion with a meso hydroxyl group.

^{1}H NMR spectroscopy of iron porphyrins has been shown to be valuable in identifying the spin, ligation, and oxidation states of these complexes in reacting chemical models and in intact proteins.[9,10] Here we present an analysis of the ^{1}H NMR spectra of iron(III) oxophlorin complexes that are derived from octaethylporphyrin. The work begins with the novel iron(III) oxophlorin dimer **3** (a–d = ethyl, m and m′ = hydrogen), $[Fe^{III}$-

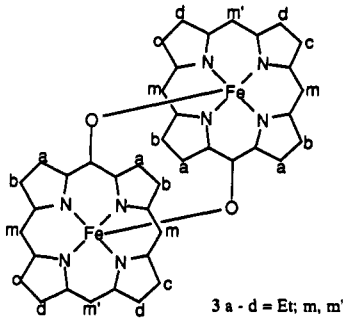

3 a - d = Et; m, m' = H.

$(OEPO)]_2$, initially characterized by Masuoko and Itano.[11] In this neutral, centrosymmetric dimer the oxophlorins are present as trianions with the meso oxygen of one acting as a donor toward the iron ion at the center of the other oxophlorin. This complex differs from the ubiquitous "μ-oxo dimers" found in iron-porphyrin chemistry in that there is no oxo group present.[12] Magnetic susceptibility data indicate that **3** is antiferromagnetic but that the coupling is weak ($J = -12$ cm^{-1})[11] when compared to porphyrin μ-oxo dimers ($J \sim -130$ cm^{-1}).

Results

^{1}H NMR Spectroscopic Studies of $[Fe^{III}(OEPO)]_2$ (3). Samples of $[Fe^{III}(OEPO)]_2$ have been prepared by a new route that involves

(1) Clezy, P. S. In *The Porphyrins*; Dolphin, D., Ed.; Academic Press: New York, 1978; Vol. II, p 103.
(2) O'Carra, P. In *Porphyrins and Metalloporphyrins*; Smith, K. M., Ed.; Elsevier: Amsterdam, 1976; p 123.
(3) Coupled oxidation involves oxidation of an iron porphyrin, usually in pyridine solution, with dioxygen as oxidant and a second co-oxidized reductant which is generally ascorbic acid or hydrazine.
(4) Bonnett, R.; Dimsdale, M. J. *J. Chem. Soc. Perkin Trans. 1* **1972**, 2540.
(5) Drummond, G. S.; Kappas, A. *Proc. Natl. Acad. Sci. U.S.A.* **1981**, *78*, 6466.
(6) Kappas, A.; Drummond, G. S.; Manola, T.; Petmezaki, S.; Valaes, T. *Pediatrics* **1988**, *81*, 485.
(7) Fuhrhop, J.-H.; Besecke, S.; Subramanian, J. *J. Chem. Soc., Chem. Commun.* **1973**, 1. Fuhrhop, J.-H.; Besecke, S.; Subramanian, J.; Mengersen, C.; Riesner, D. *J. Am. Chem. Soc.* **1975**, *97*, 7141.
(8) Balch, A. L.; Noll, B. C.; Zovinka, E. P. *J. Am. Chem. Soc.* **1992**, *114*, 3380.
(9) Latos-Grażyński, L.; Balch, A. L.; La Mar, G. N. *Adv. Chem. Ser.* **1982**, *No. 201*, 661.
(10) La Mar, G. N.; Walker (Jensen), F. A. In *The Porphyrins*; Dolphin, D., Ed.; Academic Press: New York 1978; Vol. IV, p 61.
(11) Masuoka, N.; Itano, H. A. *Biochemistry* **1987**, *26*, 3672.
(12) Murray, K. S. *Coord. Chem. Rev.* **1974**, *12*, 1.

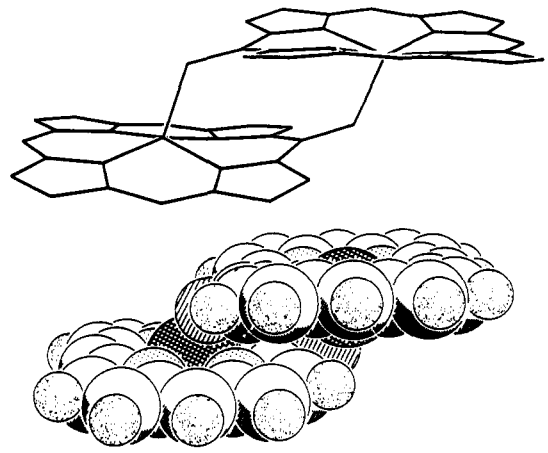

Figure 1. Drawings of the dimer **3** with a–d = H and m, m′ = H obtained from molecular mechanics calculations. The top shows a stick diagram with hydrogen atoms omitted while the bottom shows a space filling model that includes the hydrogen atoms.

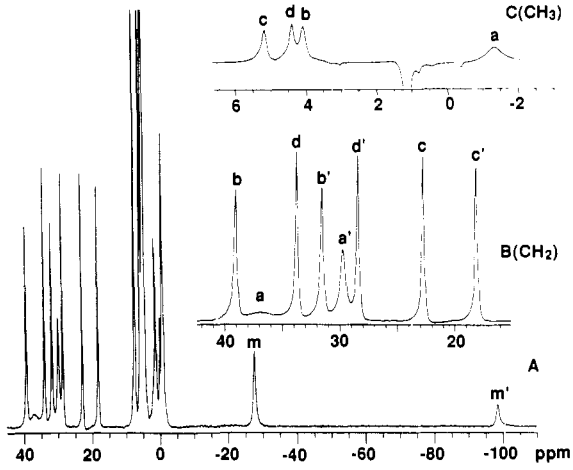

Figure 2. 300-MHz ^{1}H NMR spectra of $[Fe^{III}(OEPO)]_2$ in chloroform-*d* at 28 °C. Trace A is the entire spectrum while B shows an expansion of the methylene resonances. Trace C shows the −3 to +6 ppm region obtained by selective inversion of diamagnetic peaks with the rapidly relaxing paramagnetic resonances appearing in the normal phasing. Individual resonance assignments to specific protons in the oxophlorin structure **1** are explained in the text.

metalation of octaethyloxophlorin, **1** (a–d = ethyl; m, m′ = hydrogen),[13] with chromatographic separation of the products. The spectroscopic properties and chemical behavior of the material obtained this way are identical with those reported previously.[11] Extensive attempts to obtain this compound as crystals suitable for X-ray crystallographic study have not been successful. In the absence of those data, molecular mechanics calculations have been used to visualize the structure of the dimer and to access the degree of distortion of the macrocycle that is necessary to form this species. The results are shown in Figure 1. As can be seen, only moderate folding of the macrocycle and bending of the oxo substituent out of the plane are required.

Figure 2 shows ^{1}H NMR spectra of $[Fe(OEPO)]_2$ (**3**) in chloroform-d_1 at 28 °C. Resonance positions are given in Table II. Trace A of Figure 2 shows the entire spectrum. The resonances can be separated into three groups and assigned to functional groups on the basis of their relative intensities and the number of resonances observed. The two types of meso protons produce two resonances in the upfield region which can be assigned to m and m′ on the basis of their intensities. The methylene protons produce resonances in the 40 to 18 ppm region, while the methyl protons give resonances in the 6 to −2 ppm region. Inset

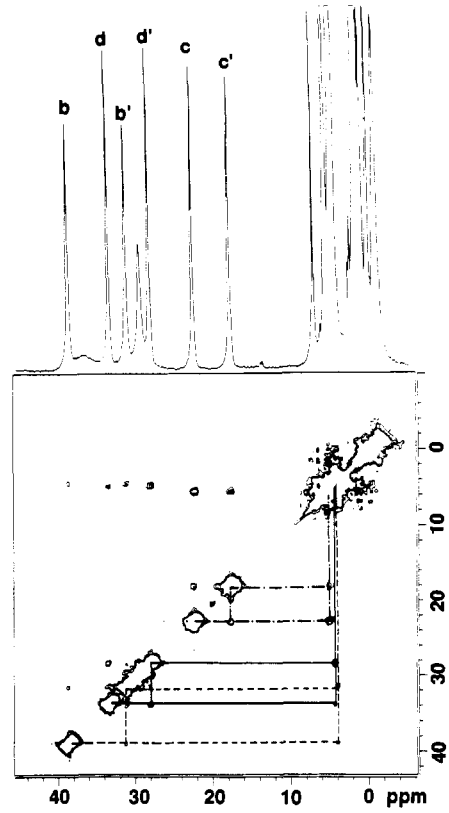

Figure 3. (Top) A portion of the 300-MHz ^{1}H NMR spectrum of $[Fe^{III}(OEPO)]_2$ in chloroform-*d* at 25 °C. (Bottom) 300-MHz MCOSY plot for $[Fe^{III}(OEPO)]_2$. Cross peaks connecting the three resonances of three of the four ethyl groups, b–d, are shown. Resonance assignments follow those in Figure 2.

B shows an expansion of the methylene region. Eight individual resonances are present. One of these (a) is very broad and another (a′) is noticeably broader than the other six. Peaks labeled b and b′ are shorter and therefore broader than the remaining four peaks, c–d′. The observation of eight methylene resonances is consistent with the dimeric structure **3** of this complex. Dimerization makes one side of the oxophlorin ring inequivalent to the other. Consequently, the methylene protons on any one ethyl group are diastereotopic. Inset C shows an expansion of the methyl region. This spectrum is taken under conditions that invert resonances of all diamagnetic peaks but not those of the rapidly relaxing resonances. As a result, the four peaks labeled a–d in inset C can be assigned to a (paramagnetic or weakly antiferromagnetic) entity despite the fact that they lie within the diamagnetic region. The occurrence of four equally intense resonances correlates with expectations based on sturcture **3** where four methyl environments (a–d) exist. The most upfield of these resonances, labeled a, is the broadest and can be associated with the broadest of the methylene resonances (a and a′) in inset B.

Two-dimensional magnitude COSY (MCOSY) experiments have been shown to be effective in connecting the protons within ethyl groups in paramagnetic molecules.[14] Within each ethyl group, the methylene and methyl protons are expected to be coupled with an approximate 14-Hz coupling for geminal and 7-Hz coupling for vicinal protons. Cross peaks connecting two methylene proton resonances and one methyl resonance should be detectable. Figure 3 shows MCOSY data gathered from a chloroform-d_1 solution of $[Fe^{III}(OEPO)]_2$ at 25 °C. Cross peaks reveal pairwise coupling between six of the methylene resonances, and further cross peaks connect these pairs with the three downfield methyl resonances. The results of these assignments were used to identify the individual resonances in Figure 2 and the resonance positions are given in Table II. Thus methylene

(13) Barnett, G. H.; Hudson, M. F.; McCombie, S. W.; Smith, K. M. *J. Chem. Soc., Perkin Trans. 1* **1973**, 691.

(14) Keating, K. A.; de Ropp, J. S.; La Mar, G. N.; Balch, A. L.; Shiau, F.-Y.; Smith, K. M. *Inorg. Chem.* **1991**, *30*, 3258.

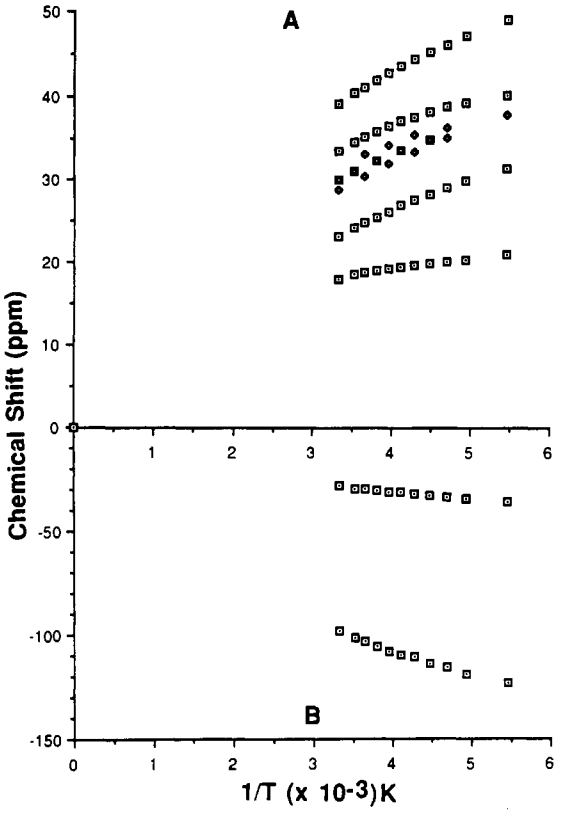

Figure 4. Curie plots of the chemical shifts of the methylene (A) and meso (B) resonances of $[Fe^{III}(OEPO)]_2$.

resonances b and b′ in trace B and methyl resonance b in trace C of Figure 2 are connected by appropriate cross peaks, etc. Not unexpectedly, no cross peaks are seen for the broad methylene resonances (a and a′) and the broad methyl resonance (a), but these can be assigned by default.

In order to assess the cause of the marked variation of line widths seen for $[Fe^{III}(OEPO)]_2$, T_1 data for all of its resonances (Figure 2) have been obtained. The results are as follows: methylene protons a, 0.3 ms; a′, 2.1; b, 7.5; b′, 7.1; c, 14.6; c′, 11.5; d, 16.7; d′, 15.1; methyl protons a, 2.5 ms; b, c, and d, 16.9 ms; meso protons m, 2.2 ms; m′, 1.7. Notice that for the methylene protons, the T_1 values for pairs of protons which have been assigned to a common ethyl group have similar magnitudes. These T_1 values have been used to correlate individual resonances with proton location within the dimeric structure. The dipolar contribution to T_1 is presumed to be proportional to r^{-6}, where r is the distance from the iron to the proton in question.[15] The key assumption which has been made is that the iron center coordinated to the meso-oxygen produces a local relaxation effect that enhances the T_1 values for protons that are closest to that meso oxygen. This allows mapping of the individual methylene protons so that a and a′ are closest to that oxygen and d and d′ are furthest from it. As confirmation of this assumption, notice that T_1 for the m protons, which are uniquely defined on the basis of their intensity, is lower than for the m′ proton. Calculations have been made which give the ratios of the dipolar contribution to the T_1's for the protons in $[Fe^{III}(OEPO)]_2$ that result from the second paramagnetic center, the meso Fe–O unit. These have been made with a model which uses the structure of $ClFe^{III}(OEPOC(O)CH_3)$ (vide infra) and an iron ion replacing the $C(O)CH_3$ group and an Fe–O distance of 1.7 Å. This model gives a set of relative T_1 contributions for $a(CH_2)$, $a'(CH_2)$, $a(CH_3)$, $b(CH_2)$, and $b'(CH_2)$ of 0.05:1:1.1:7.0:16 while the experimental values are 0.14:1:1.2:3.6:3.4. The model assumes a static structure in which the proton locations are fixed. Considering the simplicity of this model, the agreement in predicting the trends in T_1 is reasonable.

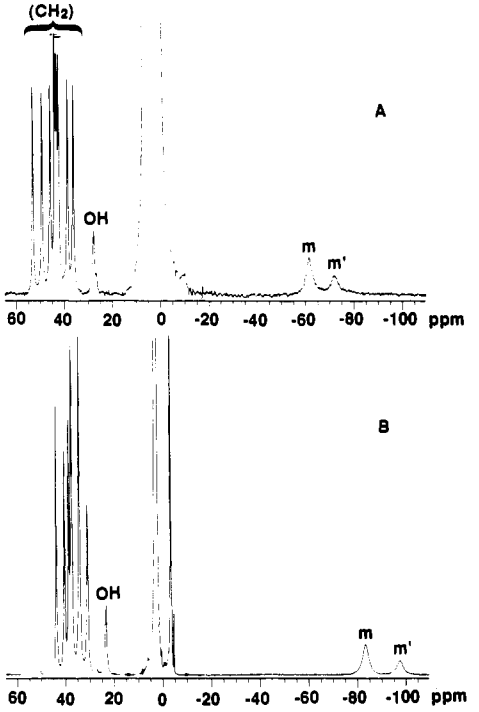

Figure 5. 300-MHz ^1H NMR spectra of $[Fe^{III}(OEPO)]_2$ after treatment with (A) trifluoroacetic acid at 23 °C and (B) hydrogen bromide at 25 °C in chloroform-*d*. The species present in A is $(CF_3CO_2)Fe^{III}(OEPOH)$ and in B is $BrFe^{III}(OEPOH)$. Resonance assignments follow those in Figure 2 with OH indicating the meso-hydroxyl proton.

The temperature dependence of the ^1H NMR spectrum of $[Fe^{III}(OEPO)]_2$ is shown in Figure 4 where the chemical shifts of the methylene and meso protons are plotted versus $1/T$. As is apparent, these plots are not linear but are slightly curved. Slight curvature in such plots is found for many high-spin iron(III) porphyrin complexes.[16,17] The curvature of monomeric complexes originates in the zero field splitting present in the $S = {}^5/_2$ species. However, in Figure 4 the direction of curvature is opposite that found for monomeric iron(III) complexes.[16,17] The reversed curvature seen in Figure 4 is consistent with the presence of weak antiferromagnetic coupling between the two iron ions within the dimer. Similarly curved plots of chemical shift versus $1/T$ have been observed for weakly coupled iron(III) dimers with hydroquinone dianionic bridges.[18]

Cleavage of $[Fe^{III}(OEPO)]_2$ by Protic Acids. Addition of acids to $[Fe^{III}(OEPO)]_2$ results in cleavage of the dimer according to eq 1. Figure 5 shows relevant ^1H NMR spectra. The spectrum

$$[Fe^{III}(OEPO)]_2 + 2HX \rightleftharpoons 2XFe^{III}(OEPOH)\ (\mathbf{4}) \quad (1)$$

in trace A shows a sample of $[Fe^{III}(OEPO)]_2$ to which trifluoroacetic acid has been added. The spectrum is consistent with the formation of $(CF_3CO_2)Fe^{III}(OEPOH)$ (**4**). Two meso resonances are observed in the upfield region. Eight methylene resonances are found in the 55–35 ppm region. These have nearly equal line widths. The differential broadening of resonances that is characteristic of $[Fe^{III}(OEPO)_2]$ is absent. The observation of eight methylene resonances is readily explained if a single axial ligand (in this case trifluoroacetate) is coordinated to the iron. A unique resonance at 28 ppm is assigned to the meso hydroxyl proton of $(CF_3CO_2)Fe^{III}(OEPOH)$. When CF_3COOD is used for the preparation of this complex, the resonance at 28 pm is not observed. Reaction 1 is reversible. Addition of a base to $(CF_3CO_2)Fe^{III}(OEPOH)$ causes its reversion to $[Fe^{III}(OEPO)]_2$.

(15) Swift, T. J. In *NMR of Paramagnetic Molecules*; La Mar, G. N., Horrocks, W. D., Jr., Holm, R. H., Eds.; Academic Press: New York, 1973; p 53.

(16) Walker, F. A.; La Mar, G. N. *Ann. N.Y. Acad. Sci.* **1973**, *206*, 328.

(17) La Mar, G. N.; Eaton, G. R.; Holm, R. H.; Walker, F. A. *J. Am. Chem. Soc.* **1973**, *95*, 63.

(18) Balch, A. L.; Hart, R. L., Latos-Grażyfiski, L. *Inorg. Chem.* **1990**, *29*, 3253.

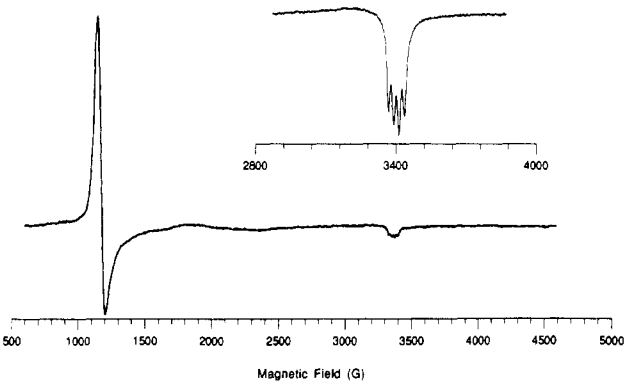

Figure 6. Electron spin resonance spectrum of $BrFe^{III}$(OEPOH) in chloroform-*d* at 8 K.

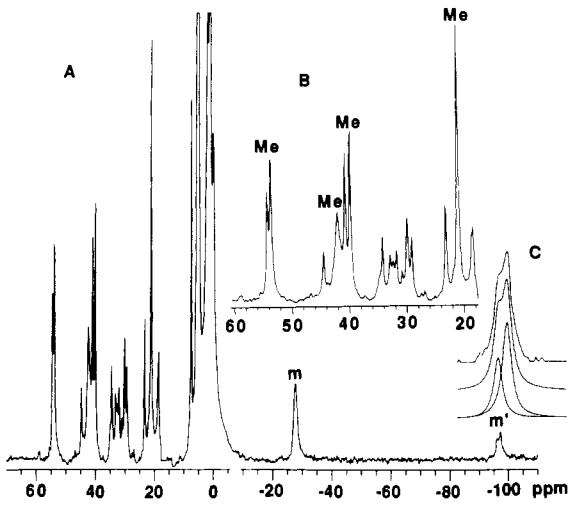

Figure 7. ^{1}H NMR spectra of $[Fe^{III}$(Etio I O)$]_2$ in chloroform-*d* at 25 °C. Trace A shows the entire spectrum. Trace B shows an expansion of the methyl and methylene proton resonances; pyrrole methyl resonances are identified as Me. Trace C shows an expansion of the m proton resonances and their deconvolution to show the presence of two isomers.

Thus addition of collidine (2,4,6-trimethylpyridine, a noncoordinating base) to the sample whose ^{1}H NMR spectrum is shown in trace A of Figure 5 results in the lose of these peaks and the growth of the resonances shown in Figure 2 for $[Fe^{III}(OEPO)]_2$.

Trace B of Figure 5 shows the effect of the addition of hydrogen bromide to $[Fe^{III}(OEPO)]_2$. The spectrum of the product, $BrFe^{III}$(OEPOH) (**4**) (X = Br) is similar to that of the trifluoroacetate analogue. The two upfield meso resonances and the OH resonance at 28.2 ppm are clearly observed. In the methylene region, some of the resonances overlap so that four resonances due to two protons each are seen along with two resonances due to four protons apiece. Methyl resonances occur at 1.4 and 7.5 ppm. Data for products obtained by cleavage of $[Fe^{III}(OEPO)]_2$ by other acids including hydrogen chloride are given in Table II. All show a similar pattern for the oxophlorin resonances. In each case, the observation of a hydroxyl proton resonance ensures us that the tetrapyrrole ligand is present in its mono protonated form.

Figure 6 shows the electron paramagnetic resonance (EPR) spectrum obtained from a sample of $BrFe^{III}$(OEPOH) in frozen chloroform at 8 K. The spectrum is characteristic of a high-spin, five-coordinate iron(III) complex. The high-field line shows well-resolved hyperfine splitting which is due to Fe–Br coupling with a = 28 G. The four-line pattern is consistent with the presence of one bromide (^{79}Br, 50.5%; ^{81}Br, 49.5% natural abundance; both spin $^3/_2$) as an axial ligand. The magnitude of the Fe–Br coupling constant is the same that is seen in bromoiron(III) protoporphyrin.[19]

(19) Van Camp, H. L.; Scholes, C. P.; Mulks, C. F. *J. Am. Chem. Soc.* **1976**, *98*, 4094.

^{1}H NMR Studies of $[Fe^{III}$(Etio I O)$]_2$. The spectroscopic properties of iron(III) complexes of the oxophlorin **5**, which is

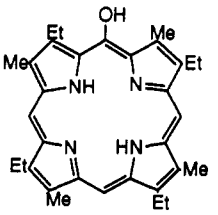

5 (Etio I OH_3)

derived from etioporphyrin I, have been examined in order to identify pyrrole methyl chemical shifts and to verify the structural consequences of the lower symmetry of this substance. Figure 7 shows ^{1}H NMR spectra of Fe^{III}(Etio I O) in chloroform-d_1. Trace A shows the full spectrum. The pattern is similar to that seen for $[Fe^{III}(OEPO)]_2$ with a large difference in the chemical shifts of the m and m′ protons. Trace B shows an inset for the m′ protons. Clearly two overlapping resonances are present. These are due to the presence of two dimers **6** (M = methyl, E = ethyl,

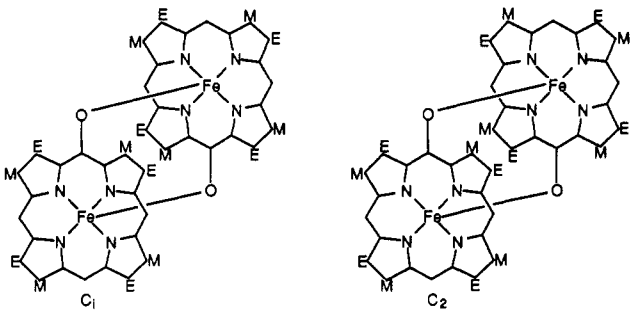

double bonds omitted for clarity) with C_i symmetry and **7** with C_2 symmetry. In each dimer the two m′ protons are equivalent but the presence of two distinct dimers with unequal concentration produces two resonances. The other meso protons in the oxophlorin **5** are also inequivalent, but the difference, which involves the orientation of the adjacent methyl and ethyl groups, is more subtle and no differentiation is seen in the spectrum in Figure 7 despite the fact that four distinct m sites are present, two in each of the dimers **6** and **7**. Inset C shows an expansion of the region of methyl and methylene resonances. The spectrum in this region is complex and cannot be explained by the presence of a single species. Because of apparent overlapping of some resonances, only a tentative analysis of the entire region can be made. Four methyl resonances are expected for each dimer. One of these (the one corresponding to the methyl group adjacent to the meso oxygen and closest to the Fe–O paramagnetic center) is expected to be significantly broader than the others. The intense resonances denoted Me in trace C of Figure 7 are assigned to the methyl groups. The assignment of resonances downfield of 40 ppm to the methyl groups is further strengthened by the observation that $[Fe^{III}(OEPO)]$ has no resonances beyond 40 ppm. Notice that the most downfield feature that we assign to a methyl group appears as two resonances of unequal intensity and that there are two unequal components to the resonance at 39 ppm. These we believe are due to the presence of the two different isomers **6** and **7** which will produce two sets of four methyl resonances. The other resonances in this region are due to the methylene protons. Up to 16 resonances (two sets of eight) are expected.

Addition of protic acids to $[Fe^{III}$(Etio I O)$]_2$ results in a notable simplification of the spectrum as seen in Figure 8. Trace A shows the full spectrum in chloroform-*d* at −20 °C. Two meso resonances occur in the −90 and −110 ppm region. The methyl and methylene resonances occur in the 75 to 30 ppm region. The meso OH group produces a broad resonance at 20 ppm. This resonance disappears when the sample is shaken with deuterium oxide and moves upfield on warming. Inset B shows an expansion of the downfield region at 23 °C. Four methyl resonances and eight less intense methylene resonances are clearly resolved. The spectrum is consistent with

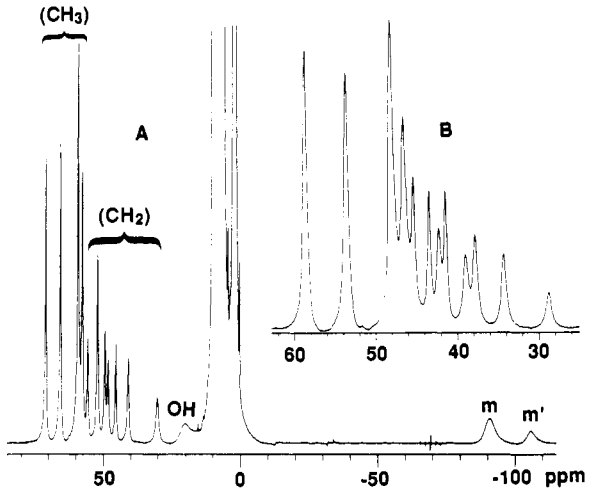

Figure 8. ^{1}H NMR spectrum of $[Fe^{III}(Etio\ I\ OH)]_2$ in chloroform-*d* after the addition of hydrogen chloride. Trace A is the full spectrum at −20 °C. Trace B shows the methyl and methylene proton resonances at 23 °C.

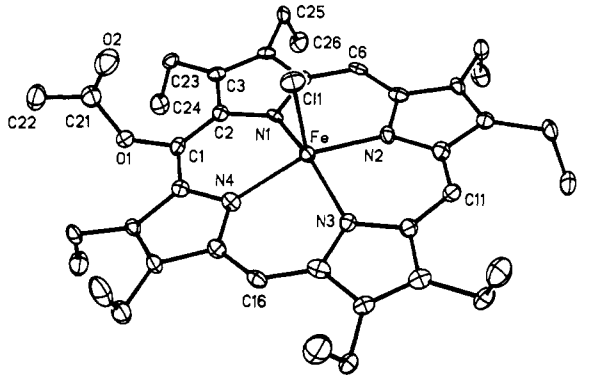

Figure 9. A perspective view of $ClFe^{III}$(OEPOAc) with 50% thermal contours.

the presence of high-spin, five-coordinate $BrFe^{III}$(Etio I OH).

Crystal and Molecular Structure of $ClFe^{III}$(OEPOAc)·CH_2Cl_2 (8) (X = Cl). Metalation of *meso*-acetoxyoctaethylporphyrin with iron(III) chloride yields $ClFe^{III}$(OEPOAc). The structure of this complex has been determined by X-ray crystallography. As crystallized from dichloromethane, the asymmetric unit consists of the iron complex and a disordered molecule of dichloromethane with no unusual contacts between these.

The structure of $ClFe^{III}$(OEPOAc) is shown in Figure 9. Selected interatomic distances and angles are given in Table III. The complex has no crystallographically imposed symmetry. The iron has the geometric structure typical for a high spin ($S = {}^5/_2$), five-coordinate complex.[20,21] Thus the Fe–N distances (2.060–2.075 Å) fall in the range (2.060–2.087 Å) expected for this class. Similarly, the distance of the iron from the N_4 plane (0.46 Å) is also in the range 0.39–0.54 Å that is found for high-spin, five-coordinate iron(III) porphyrin complexes. The Fe–Cl distance 2.236 (2) Å is similar to the Fe–Cl distances in $ClFe^{III}$(protoporphyrin IX dimethyl ester) (2.218 (6) Å)[22] and somewhat longer than the distances in $ClFe^{III}$(TPP) (2.192 (12) Å)[23] and in $[ClFe^{III}(N\text{-MeTPP})](SbCl_6)$ (2.164 (3) Å).[24]

The acetoxy group does not produce a profound effect on the overall porphyrin structure. However, the region around the acetoxy group itself is quite crowded. This is best seen by turning to Figure 10 where the molecule is shown with atomic contours that represent van der Waals radii. The molecule is oriented so that the acetoxy group faces the reader. The carbonyl oxygen and the chloride ligand lie on the same face of the porphyrin. Rotation of the acetoxy group about the C(meso)–O bond is restricted by the two ethyl groups that flank the acetoxy substituent. Hence, there are two possible isomeric forms of this

Table III. Bond Lengths and Angles for $ClFe^{III}$(OEPOAc)

Bond Lengths (Å)			
Fe–Cl(1)	2.236 (2)	Fe–N(1)	2.073 (5)
Fe–N(2)	2.060 (4)	Fe–N(3)	2.075 (4)
Fe–N(4)	2.066 (4)	O(1)–C(1)	1.421 (6)
O(1)–C(21)	1.376 (7)	O(2)–C(21)	1.194 (9)
N(1)–C(2)	1.397 (6)	N(1)–C(5)	1.379 (6)
N(2)–C(7)	1.388 (6)	N(2)–C(10)	1.380 (7)
N(3)–C(12)	1.380 (6)	N(3)–C(15)	1.387 (6)
N(4)–C(17)	1.382 (6)	N(4)–C(20)	1.387 (7)
C(1)–C(2)	1.394 (6)	C(1)–C(20)	1.386 (7)
C(2)–C(3)	1.450 (7)	C(3)–C(4)	1.367 (6)
C(4)–C(5)	1.442 (7)	C(5)–C(6)	1.374 (6)
C(6)–C(7)	1.388 (7)	C(7)–C(8)	1.450 (6)
C(8)–C(9)	1.360 (7)	C(9)–C(10)	1.445 (7)
C(10)–C(11)	1.381 (7)	C(11)–C(12)	1.384 (7)
C(12)–C(13)	1.450 (7)	C(13)–C(14)	1.354 (7)
C(14)–C(15)	1.454 (7)	C(15)–C(16)	1.377 (7)
C(16)–C(17)	1.381 (8)	C(17)–C(18)	1.434 (7)
C(18)–C(19)	1.364 (8)	C(19)–C(20)	1.450 (6)
Bond Angles (deg)			
Cl(1)–Fe–N(1)	101.1 (1)	Cl(1)–Fe–N(2)	102.4 (1)
N(1)–Fe–N(2)	87.9 (2)	Cl(1)–Fe–N(3)	103.9 (1)
N(1)–Fe–N(3)	154.9 (2)	N(2)–Fe–N(3)	86.2 (1)
Cl(1)–Fe–N(4)	104.2 (1)	N(1)–Fe–N(4)	86.2 (2)
N(2)–Fe–N(4)	153.4 (2)	N(3)–Fe–N(4)	88.1 (2)
C(1)–O(1)–C(21)	116.5 (5)	Fe–N(1)–C(2)	127.9 (3)
Fe–N(1)–C(5)	124.5 (3)	C(2)–N(1)–C(5)	105.8 (4)
Fe–N(2)–C(7)	126.2 (3)	Fe–N(2)–C(10)	127.3 (3)
C(7)–N(2)–C(10)	105.2 (4)	Fe–N(3)–C(12)	127.4 (3)
Fe–N(3)–C(15)	125.9 (3)	C(12)–N(3)–C(15)	105.2 (4)
Fe–N(4)–C(17)	124.8 (4)	Fe–N(4)–C(20)	128.6 (3)
C(17)–N(4)–C(20)	105.2 (4)	O(1)–C(1)–C(2)	115.8 (4)
O(1)–C(1)–C(20)	115.0 (4)	C(2)–C(1)–C(20)	129.1 (5)
N(1)–C(2)–C(1)	121.8 (5)	N(1)–C(2)–C(3)	109.9 (4)
C(1)–C(2)–C(3)	128.3 (5)	C(2)–C(3)–C(4)	106.5 (4)
C(3)–C(4)–C(5)	107.5 (4)	N(1)–C(5)–C(4)	110.2 (4)
N(1)–C(5)–C(6)	125.8 (5)	C(4)–C(5)–C(6)	123.9 (4)
C(5)–C(6)–C(7)	126.6 (4)	N(2)–C(7)–C(6)	124.1 (4)
N(2)–C(7)–C(8)	110.3 (4)	C(6)–C(7)–C(8)	125.5 (4)
C(7)–C(8)–C(9)	106.8 (4)	C(8)–C(9)–C(10)	106.9 (4)
N(2)–C(10)–C(9)	110.7 (4)	N(2)–C(10)–C(11)	124.7 (4)
C(9)–C(10)–C(11)	124.6 (5)	C(10)–C(11)–C(12)	126.5 (5)
N(3)–C(12)–C(11)	123.5 (5)	N(3)–C(12)–C(13)	110.4 (4)
C(11)–C(12)–C(13)	126.0 (5)	C(12)–C(13)–C(14)	107.4 (4)
C(13)–C(14)–C(15)	106.4 (4)	N(3)–C(15)–C(14)	110.6 (4)
N(3)–C(15)–C(16)	123.7 (5)	C(14)–C(15)–C(16)	125.7 (4)
C(15)–C(16)–C(17)	127.6 (5)	N(4)–C(17)–C(16)	125.4 (4)
N(4)–C(17)–C(18)	110.3 (4)	C(16)–C(17)–C(18)	124.3 (4)
C(17)–C(18)–C(19)	107.9 (4)	C(18)–C(19)–C(20)	105.7 (4)
N(4)–C(20)–C(1)	122.1 (4)	N(4)–C(20)–C(19)	110.7 (4)
C(1)–C(20)–C(19)	127.1 (5)	O(1)–C(21)–O(2)	121.9 (5)
O(1)–C(21)–C(22)	111.0 (6)	O(2)–C(21)–C(22)	127.1 (5)

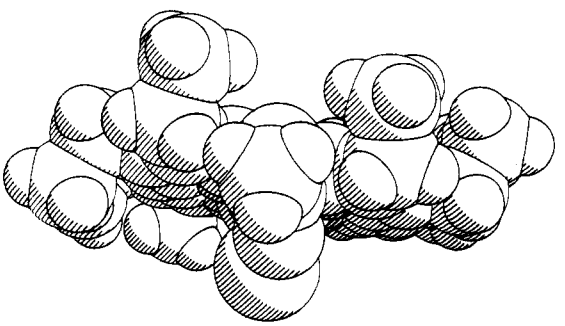

Figure 10. A view of $ClFe^{III}$(OEPOAc) looking at the acetoxy group. Space-filling van der Waals contours are shown.

(20) Scheidt, W. R.; Reed, C. A. *Chem. Rev.* **1981**, *81*, 543.
(21) Scheidt, W. R.; Lee, Y. J. *Struct. Bonding* **1987**, *64*, 1.
(22) Koenig, D. F. *Acta Crystallogr.* **1965**, *18*, 663.
(23) Hoard, J. L.; Cohen, G. H.; Glick, M. D. *J. Am. Chem. Soc.* **1967**, *89*, 1992.
(24) Balch, A. L.; Cornman, C. R.; Latos-Grażyński, L.; Olmstead, M. M. *J. Am. Chem. Soc.* **1990**, *112*, 7552.

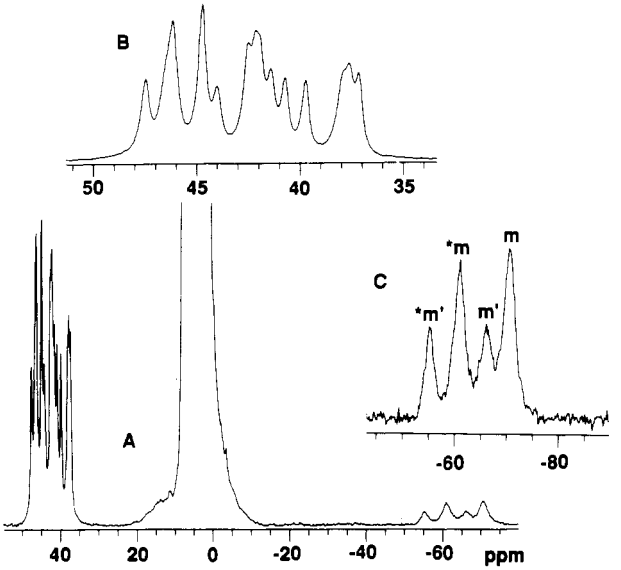

Figure 11. (A) 300-MHz ^{1}H NMR spectrum of BrFe(OEPOAc) in chloroform-d_1 at 23 °C. Trace B shows an expansion of the methylene region while trace C shows an expansion of the meso region.

complex: one with the carbonyl oxygen and the chloride on the same side of the porphyrin, **8**; and one with these groups on opposite faces of the porphyrin plane, **9**. In solution, interconversion between these can occur by the dissociation and rebinding of a chloride to the opposite face or by rotation about the C(meso)–O bond. In the solid only isomer **8** is present.

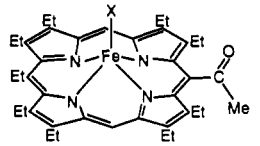

8

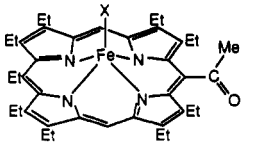

9

^{1}H NMR Studies of XFe^{III}(OEPOAc). As a model for high-spin, five-coordinate iron(III) monomers, we have examined the NMR spectral characteristics of iron(III) complexes of the *meso*-acetoxyporphyrin **3**. This has a nonlabile group bound to the oxygen at the meso position, so it should provide a model for the oxygen-protonated form of the tetrapyrrole ligand. The ^{1}H NMR spectrum of BrFe^{III}(OEPOAc) in chloroform-d_1 at 23 °C is shown in Figure 11. While the overall spectrum shown in trace A is similar to those shown in Figure 3, it has important differences. In the meso region, which is shown expanded in inset C, there are four, rather than two, resonances. Resonances m and m′ have a 2:1 intensity ratio as do *m and *m′. In different preparations of BrFe^{III}(OEPOAc) the relative intensities of the m and *m set of peaks vary. This is consistent with the presence of two isomers: one with the axial bromide and the acetoxy group on the same side of the oxophlorin plane, the other with these on opposite sides as shown in **8** and **9**, respectively. No resonances are seen in the 20–35 ppm region where the OH protons produce resonances in **4**, since BrFe^{III}(OEPOAc) lacks an OH substituent. There are at least 11 peaks in the region where methylene proton resonances are expected (inset **B**). Eight equally intense methylene resonances are expected for each of the two isomers **8** and **9** to give a maximum of 16 expected peaks in this region. Some overlapping of resonances occurs in the region. The ^{1}H NMR spectrum of ClFe^{III}(OEPOAc) is similar but, as expected, for high-spin iron(III) the lines are broader and hence less well resolved. Nevertheless, four distinct resonances are observed in the upfield region for the meso protons. This indicates that two isomers are present in solution. Addition of collidine to samples of XFe^{III}(OEPOAc) (X = Br, Cl) does not produce [Fe^{III}(OEPO)]$_2$ but does produce some broadening of the resonances. This may be due to ligand exchange processes involving the axial ligands.

Discussion

The ^{1}H NMR spectra of the monomeric iron(III) complexes XFe^{III}(OEPOH) and XFe^{III}(OEPOAc) show patterns of resonances that are similar to the pattern seen for the porphyrin complexes XFe^{III}(OEP).[14,15] Thus the meso protons are upfield, the diastereotopic methylene protons are downfield, and the methyl resonances are near the diamagnetic region. The magnitudes of the shifts are also similar.

The NMR data offer confirming evidence that the dimeric structure of [Fe^{III}(OEPO)]$_2$ (**3**) is retained in solution. The dimer shows a pattern of resonances that is similar to the monomeric species with meso protons upfield and methylene protons downfield. However, the difference in chemical shifts for the two meso resonances in the dimer is much more pronounced. This is not unexpected in a dimeric structure in which two paramagnetic centers are contributing differently to the spin distribution.

The formation of the dimeric structure of **3** and its etioporphyrin analogue requires the close approach of the porphyrins. Porphyrins are known to readily aggregate into structures with 3.4–3.6 Å separation between the two porphyrin planes.[20,21,25] Formation of the meso-oxygen bridges almost certainly requires some distortion at the meso carbon. It is likely that the meso oxygen will be pulled appreciably out of the plane of the oxophlorin toward the adjacent iron as seen in Figure 1. Complexes in which a porphyrin *N*-oxide acts as an axial ligand toward a metalloporphyrin produce good structural models for dimeric **3**.[26] In (OEP)Mn(OEPH$_2$-*N*-oxide) the plane of the porphyrin and the porphyrin *N*-oxide are separated by 3.34 Å but the manganese ion is only 0.148 Å out of the porphyrin plane.[26] The longer out-of-plane distance (ca. 0.40 Å) expected for iron in **3** will somewhat alleviate the need for close approach of the two oxophlorin ligands.

The acid/base chemistry observed for the dimer **3** shown in eq 1 is similar to that seen for a related dimer of Goff and co-workers, [Fe^{III}(TTOP)$_2$] (TTOP is the dianion of 5-(2-hydroxyphenyl)-10,15,20-tritolylporphyrin).[27] In this novel dimer one of the meso substituents provides a phenolate bridge to the iron ion in an adjacent porphyrin. Like **3**, this dimer shows very weak antiferromagnetic coupling with $|J|$ less than 5 cm^{-1}. It, too, is readily cleaved by protic acids to give high-spin, five-coordinate monomers XFe^{III}(TTOHP).

Finally we note that all of the complexes studied here are stable to molecular oxygen. Under the conditions used to handle them and to obtain the spectra shown here, there was no evidence for their conversion into verdoheme. It is apparent that protonation or coordination of the meso oxygen of the iron oxophlorin stabilized these complexes against ligand oxidation. Further work on the formation of verdoheme and its structure will appear separately.

Experimental Section

Preparation of Compounds. Octaethyloxophlorin (**1**) (a–d = ethyl, m, m′ = hydrogen),[13] etioporphyrin I oxophlorin,[13] and *meso*-acetoxyoctaethylporphyrin (**2**) were prepared by established routes.

[Fe^{III}(OEPO)]$_2$. A slurry of 17 mg of anhydrous iron(III) chloride and 300 mg of iron powder in 25 mL of tetrahydrofuran was heated under reflux for 3 h under a dinitrogen atmosphere. Octaethyloxophlorin (40 mg) and 0.1 mL of collidine were added. The solution immediately became red. The solution was cooled to room temperature and then filtered through a bed of celite. Solvent was removed from the filtrate with a rotary evaporator. The sample was dried under vacuum for 12 h. The complex was purified by dissolution in dichloromethane and chromatography on a 13 cm by 2.2 cm column of silica gel using dichloromethane as the eluant. The first red band contained the desired complex. That band was collected and evaporated to dryness to yield the product. UV–vis (λ_{max}): 390, 490, 530, 670, 1050 nm. [Fe^{III}(Etio I O)]$_2$ was prepared similarly.

XFe^{III}(OEPOAc) (X = Br, Cl). Iron was inserted into the *meso*-acetoxyoctaethylporphyrin as described above for [Fe^{III}(OEPO)]$_2$. The

(25) Hunter, C. A.; Sanders, J. K. M. *J. Am. Chem. Soc.* **1990**, *112*, 5525.
(26) Arasasingham, R. D.; Balch, A. L.; Olmstead, M. M.; Renner, M. W. *Inorg. Chem.* **1987**, *26*, 3562.
(27) Goff, H. M.; Shimomura, E. T.; Lee, Y. J.; Scheidt, W. R. *Inorg. Chem.* **1984**, *23*, 315.

Table IV. Crystallographic Data for $ClFe^{III}(OEPOAc)\cdot CH_2Cl_2$

$C_{39}H_{48}Cl_3FeN_4O_2$	fw = 767.0
a = 10.238 (2) Å	$P\bar{1}$, triclinic
b = 13.301 (2) Å	T = 130 K
c = 15.088 (3) Å	λ(Cu Kα) = 1.54178 Å
α = 77.610 (2)°	μ(Cu Kα) = 5.574
β = 71.820 (2)°	d_{calcd}, Mg·m^{-3} = 1.360
γ = 75.430 (2)°	transm factors 0.63-0.87
Z = 2	R^a = 0.051
V = 1868.5 (6)	$R_w{}^a$ = 0.053

$^a R = \sum||F_o| - |F_c||/F_o|$ and $R_w = \sum||F_o| - |F_c||w^{1/2}/\sum|F_o w^{1/2}|$.

purple, crystalline product obtained after recrystallization from chloroform-hexane. UV-vis (λ_{max}): 388, 506, 544, 642 nm.

X-ray Crystallographic Studies. A suitable crystal of $ClFe^{III}(OEPOAc)\cdot CH_2Cl_2$ was obtained by slow diffusion of hexane through a 2-mm layer of methanol into a dichloromethane solution of the complex in a 5 mm diameter tube. A crystal was mounted on a glass fiber with silicone grease and positioned in the cold stream of a Siemens P3/RA diffractometer. Only random fluctuations (<2%) in the intensities of two standard reflections were observed during the course of data collection. Crystal data are given in Table IV. The usual corrections for Lorentz and polarization effects were applied. Structural solution and refinement were performed with the programs of SHELXTL PLUS. Scattering factors and corrections for anomalous dispersions were taken from a standard source.[28]

The structure was solved by a Patterson synthesis and refined by full-matrix least squares. Hydrogen atoms were included at calculated positions with the use of a riding model with a C-H distance of 0.96 Å and $U_H = 0.020U_C$ Å^2. An absorption correction was applied.[29] Final refinement was carried out with anisotropic parameters for all non-hydrogen atoms. The largest feature in the final difference map was 0.52 e Å^{-3}.

Instrumentation. ^{1}H NMR spectra were recorded on a General Electric QE-300 FT spectrometer operating in the quadrature mode (^{1}H frequency is 360 MHz). The spectra were collected over a 50-kHz bandwidth with 16k data points and a 10-μs 90° pulse. For a typical spectrum, between 1000 and 5000 transients were accumulated with a 50-ms delay time. The signal-to-noise ratio was improved by apodization of the free induction decay. The residual ^{1}H spectrum of $CDCl_3$ or CD_2Cl_2 were used as a secondary reference. To obtain unambiguous methyl assignments in the diamagnetic region and T_1 values, an inversion recovery sequence was used with τ values varying between 0.5 and 100 ms.

The MCOSY spectrum was obtained after collecting a standard 1D reference spectrum. The 2D spectrum was collected by use of 1024 points in t_2 over the desired bandwidth (to include all desired peaks) with 258 t_1 blocks and 1024 scans per block. All experiments included four dummy scans prior to collection of the first block.

Figure 1 was obtained by using the program PCMODEL (Serena Software, Bloomington, IN).

Acknowledgment. We thank the National Institutes of Health (GM26226) for support, Professor G. N. La Mar and Dr. K. A. Keating for advice concerning the MCOSY spectra, and B. Sturgeon for assistance with the EPR spectrometer.

Supplementary Material Available: Tables of atomic coordinates, bond distances, bond angles, anisotropic thermal parameters, hydrogen atom postions, and crystal data for $ClFe^{III}(OEPOAc)\cdot CH_2Cl_2$ (8 pages); listings of observed and calculated structure factors (17 pages). Ordering information is given on any current masthead page.

(28) *International Tables for X-ray Crystallography*; Kynoch Press: Birmingham, England, 1974; Vol. 4.

(29) The method obtains an empirical absorption tensor from an expression relating F_o and F_c. Moezzi, B. Ph.D. Thesis, University of California, Davis, 1987.

Contribution from the Chemistry Department, Brookhaven National Laboratory, Upton, New York 11973

Syntheses, Structures, and Properties of Copper(II) and Copper(I) Complexes of the New Binucleating Ligand 1,3-Bis[bis(2-pyridylmethyl)amino]benzene

Siegfried Schindler,* David J. Szalda,*[,1] and Carol Creutz

Received August 9, 1991

The synthesis and characterization of the new copper complexes $Cu_2L'_2(H_2O)_2(ClO_4)_4\cdot 2H_2O$ (VI), $Cu_2L(H_2O)_2(ClO_4)_4\cdot 4H_2O$ (VII), $Cu_2L(CH_3CN)(PF_6)_2$ (VIII), and $Cu_2L(CO)_2(PF_6)_2$ (IX) (L = 1,3-bis[bis(2-pyridylmethyl)amino]benzene, L' = 1-[bis-(2-pyridylmethyl)amino]-3-[(2-pyridylmethyl)amino]benzene) are described. The crystal structures of the copper complexes were determined. Crystal data: complex VI, formula $Cu_2Cl_4O_{20}N_{10}C_{48}H_{54}$, triclinic space group $P\bar{1}$, Z = 1, a = 11.871 (4) Å, b = 12.313 (7) Å, c = 10.441 (14) Å, α = 108.45 (9)°, β = 102.98 (8)°, γ = 91.23 (4)°; complex VII, formula $Cu_2Cl_4O_{22}N_6C_{30}H_{40}$, orthorhombic space group, $Pmn2_1$, Z = 2, a = 23.554 (3) Å, b = 8.998 (2) Å, c = 9.863 (2) Å. The copper(II) ions in VII are bridged by a perchlorate ion in the solid state. Complex VIII of formula $Cu_2P_2F_{12}N_7C_{32}H_{31}$ crystallizes in the triclinic space group $P\bar{1}$ with Z = 2, a = 11.341 (2) Å, b = 17.421 (4) Å, c = 9.977 (2) Å, α = 93.98 (2)°, β = 106.89 (1)°, and γ = 91.47 (2)°. The two copper(I) ions in VIII are in different environments because acetonitrile is bound to only one copper site. Complex IX of formula $Cu_2P_2F_{12}O_2N_6C_{32}H_{28}$ crystallizes in the triclinic space group $P\bar{1}$ with Z = 2, a = 13.465 (2) Å, b = 15.763 (2) Å, c = 9.9839 (9) Å, α = 94.07 (1)°, β = 101.46 (1)°, and γ = 113.41 (1)°. The dicarbonyl complex IX is formed from the addition of two molecules of carbon monoxide to VIII. The binding constant for this reaction, measured at 22 ± 2 °C in dimethylformamide by cyclic voltammetry, is 2.1 × 10^8 M^{-2} per copper(I) dimer. Cyclic voltammetry and differential pulse voltammetry show that the redox potentials for $Cu^{II}Cu^{II} \rightarrow Cu^{I}Cu^{II} \rightarrow Cu^{I}Cu^{I}$ are strongly solvent dependent. Reaction of the copper(I) complex with oxygen in methanol yields the same copper(II) species as is obtained independently from the reaction of Cu^{2+} with L. Hydroxylation of the benzene ring of the ligand is not observed.

Introduction

Binuclear copper complexes have been extensively studied with the aim of simulating the active sites of the copper proteins hemocyanin and tyrosinase.[2-10] Mimicry of the proteins' reactivity toward O_2 has drawn particular interest.[6,8] However, only a few copper(I) complexes manifest this reactivity,[11-24] and at present,

(1) Permanent address: Department of Natural Sciences, Baruch College, Manhattan, NY 10010. Address questions concerning the X-ray crystallographic determinations to this author.

(2) *Copper Coordination Chemistry: Biochemical and Inorganic Perspectives*; Karlin, K. D., Zubieta, J., Eds.; Adenine Press: Guilderland, NY, 1983.

(3) Karlin, K. D.; Gultneh, Y. *J. Chem. Educ.* **1985**, *62*, 983-990.

(4) *Biological and Inorganic Copper Chemistry*; Karlin, K. D., Zubieta, J., Eds.; Adenine Press: Guilderland, NY, 1986; Vol. 1.

0020-1669/92/1331-2255$03.00/0